

## IN-SITU DETERMINATION OF THE WALL'S THERMAL PROPERTIES FOR ENERGY RETROFIT IN A COLONIAL HERITAGE BUILDING: THE CABILDO OF SALTA, ARGENTINA

Silvana FLORES-LARSEN<sup>1,\*</sup>, Marcos HONGN<sup>1</sup>, Marcelo VALDEZ<sup>1</sup>,  
Silvina GONZALEZ<sup>1</sup>, Camila GEA-SALIM<sup>1</sup>

<sup>1</sup> Instituto de Investigaciones en Energía No Convencional (INENCO) –  
Universidad Nacional de Salta – CONICET, Avenida Bolivia 5150, (4400) Salta, Argentina

### Abstract

*The energy retrofit of historic buildings requires identifying the materials and thermal properties of the building fabric. This information is essential for building energy simulation, conservation, and restoration, but, unfortunately, it is usually scarce or even non-existent in documentary sources or historical studies. This paper presents the non-destructive thermal characterization of the façade walls of the historic Cabildo of Salta, Argentina. The interdisciplinary methodology includes preliminary historical and morphological studies, identification of the masonry patterns through infrared thermography, characterization of the material thermal properties through non-destructive measurements and novel dynamical computational methods, and the integrated analysis of the results based on a cross-referencing of masonry pattern, materials, and historical data. The obtained results provide scientific support for decision making in future energy retrofit strategies and building restoration.*

**Keywords:** *In-situ thermal resistance; Infrared thermography; Wall thermal properties; Non-destructive techniques; Heritage buildings; Energy retrofit*

### Introduction

The conservation, restoration, and energy retrofit of historic buildings require identifying the materials and construction techniques used in the building fabric. In particular, energy retrofit of historical and heritage buildings has become increasingly important in recent years [1-4], driven by the energy rehabilitation campaign introduced in the European Directives on Energy Efficiency in Buildings (Directives 2010/31/EU, 2012/27/EU). Besides, building renovation is considered a key initiative in the European Green Deal to drive energy efficiency in the sector [5]. Relevant advances in the retrofit of historical buildings have been made in Europe, where the energy rehabilitation linked to heritage conservation techniques is considered one of the fundamental points towards the development of sustainable cities of the future [6-8].

Energy retrofit of heritage buildings presents huge challenges, strongly related to architectural restrictions (and artistic, in the case of frescoed walls) that oblige to preserve the building integrity of the buildings [9-12]. Another issue is the scarce information available in documentary sources or historical studies about different constructive techniques, refurbishments, and additions included in the building fabric. This information is at the base of the BES (Building Energy Simulation) that is used in the energy retrofit of heritage buildings [3].

\* Corresponding author: seflores@unsa.edu.ar

While standards and manufacturers' data sheets provide this information, the real values can be in practice very different from the theoretical ones. The main causes of this discrepancy are usually linked to unknown construction features, to the quality of materials or workmanship, the presence of voids and cracks, the moisture content, the material degradation due to ageing and outdoor exposure, the wall's inhomogeneities, etc. [13-16]. Thus, the designers, restorers, and energy simulators often face the lack of reliable thermophysical input data for the envelope components and their peculiarities [17]. Ideally, these data should be determined in-situ, as better as possible, before starting a new refurbishment or restoration work.

There are two groups of methods used to obtain this relevant information [18]: morphological analysis that describes the constructive units in the building, such as the size and shape of bricks or the building stratigraphy [19, 20], and material analysis that determines the physical, thermal, or chemical characteristics of the building materials [18, 21, 22]. For building energy simulation, the most important thermophysical properties to be determined are the thermal conductivity, the density, and the specific heat, together with the envelope characterization through its thermal transmittance (U-value) and thermal resistance (R-value). For both groups of methods, non-destructive techniques that do not damage the building structure are generally preferred to laboratory tests that require using samples from the building structure, usually taken in a destructive way.

Among the non-destructive in-situ techniques applied in energy characterization of buildings, infrared thermography and dynamical methods to determine the envelope's thermal properties are two valuable and widely applied techniques. Infrared thermography (IRT) is mainly used for addressing the morphological analysis of historical buildings [10] This technique allows a qualitative inspection of the building envelope to identify the thermal anomalies related to the presence of materials with different thermal properties (for example, stone and bricks), different thicknesses of the same material, thermal bridges, moisture, thermal insulation defects, and so on [13, 23]. On the other hand, dynamical methods allow estimating the thermal resistance or transmittance of building walls when quasi-steady standard methods cannot produce successful results, such as in non-conditioned free-running buildings, massive buildings, or heritage non-conditioned ones. In the latter, room temperatures cannot be controlled to achieve the optimal quasi-steady test conditions, such as that requiring a thermal gradient above 10°C between the outdoor and indoor air [24]. Furthermore, even when dynamical methods are used, the estimation of the thermal properties of a wall may be quite difficult and even not successful if this wall is massive and/or very thick. This situation may be encountered when analyzing stone or adobe walls usually found in heritage buildings [25].

In Latin America, historic buildings were commonly built with local materials near the construction site [26]. Thus, adobe, stones, rammed earth, mud mortar, and wood, are mostly found in walls and roofs since they were feasible alternatives those days. The mechanical properties of adobe walls have been extensively studied because they could suffer severe structural damage or even collapse when they are not well designed and strengthened. Some interesting studies were carried out on adobe buildings of the Spanish colonial times. Such studies mainly focused on the mechanical and structural requirements of the adobe constructions [27-29]. In contrast, thermal properties have been scarcely studied, and the vast majority of the investigations were performed in laboratories [30-32] or through computer simulation [33, 34]. To the authors' best knowledge, in-situ measurement of thermal properties of historic buildings have not yet been carried out in Latin America. The mainstream of research in this area was conducted in Europe and Asia. For example, in Cyprus, *Michael et al.* [35] carried out in-situ temperature monitoring of a 50cm thick adobe wall with probes installed at various locations along its thickness. In Italy, *Adhikari et al.* [15] analyzed 22 buildings (and 23 walls) in the Lombardy Region that were built during different periods between the XII-XIX centuries. The authors found that in the masonries, the differences between the theoretical and measured U-values vary considerably (from 6 to 56%). *Genova and Fatta* [25] measured the thermal

conductance of massive stone walls in a convent in Palermo, Italy. These researchers performed 16 in-situ measurements of the thermal resistance in winter and summer, with measuring periods between 6 and 21 days. They found that the weather conditions, particularly during the summer, were not stable enough to ensure a reliable estimation of the R-value. In France, *Berger and Kadoch* [36] investigated a new dynamical methodology to estimate the thermal diffusivity of a wall monitored in an old building. Their goal was two-fold: significantly reducing the computational time for solving the mathematical direct problem, and reducing the number of observations needed through optimal experiment design methodology.

From the description above, it is concluded that the in-situ determination of hygrothermal properties of historic buildings is still a developing field. In Latin America, although there is a body of literature on traditional materials and their mechanical properties, as well as the different construction techniques used in the past, there is limited or no information concerning the in-situ determination of the hygrothermal properties of historic envelope components. These hygrothermal properties have been usually overlooked compared to the mechanical ones, probably because efficient buildings and energy retrofit measures are not considered yet a main objective in the political agenda of Latin American governments.

This paper presents the in-situ non-destructive characterization of the masonry patterns and thermal properties of the façade walls of a historic building: the Cabildo of the city of Salta (Argentina). This building, today a museum, was built in the early XVI century and is regarded as the most preserved building of its type in Argentina. The building underwent a restoration campaign during the 1940 decade, but poor or no logs of the performed interventions were systematically registered. Therefore, there is little information on the materials or the constructive systems used in the original and/or the restored parts of the building. In this research, an interdisciplinary procedure for masonry identification was used that integrates historical and documentary information with two non-destructive in-situ techniques to determine the masonry patterns (infrared thermography) and the thermal properties (dynamical heat flux and surface temperature measurements) of the walls. The combination of the results obtained from different approaches is expected to produce more complete and precise information. Thermal resistance, transmittance, conductivity, thermal capacity, and thermal diffusivity were determined through in-situ measurements. These variables are of uppermost importance to study the energy retrofit of buildings. The obtained results provide scientific support for decision making in future energy retrofit strategies and building restoration.

## The case study

The city of Salta, in the northern region of Argentina, was founded in 1582. Cities founded by Spanish settlers shared a common layout: a lot in front of the main square was allocated to the Cabildo or town hall. The Cabildo was the building where the main American municipal institution operated representing the corresponding Spanish institution that, originally from the X century, counterbalanced the power of the nobility [37]. The most influential Cabildos in Argentina, such as the one in the city of Buenos Aires, had two floors and corridors around one or two patios, with the session rooms and hierarchical administrative functions arranged on the upper floor. The arcaded galleries (called “recovas”) that precede the main façade functioned as a transition space from the main square where informal neighbours’ meetings were held. The tower was a distinctive element of the Spanish architecture: it housed the bells that called the neighbours to participate in the open discussions of the Cabildo.

The building of the Cabildo of Salta was built up around the 1780s in front of the main square and it was declared Historic National Monument by the Argentinean government in 1937. Current pictures of the building and plan views of the two floors are shown in Figures 1 and 2. The main floor is characterized by large arcaded courtyards surrounded by rooms devoted to different purposes. Salta is located in a seismic zone so the historic buildings are vulnerable and

must undergo constant maintenance and restoration processes. During the 1940s major restoration works were carried out in the building by Arch. M. Buschiazzo. This restoration campaign brought to light the fact that very different construction types, probably during different periods coexisted: there are parts of the building made of adobe, with thick walls, others parts are made of brick and a large portion of stone. The Cabildo is a building with thick and massive walls (of the order of 0.5m thick or thicker) and with small openings, which corresponds to the type of design and structure of most colonial buildings of the city of Salta. The thermal characteristics of the thick adobe walls are adequate for climates with high thermal amplitudes because the thermal mass provides benefits in the sense of its thermal inertia and thermal insulation.



Fig. 1. Cabildo of Salta city. Aerial view (left) and interior main courtyard (right)

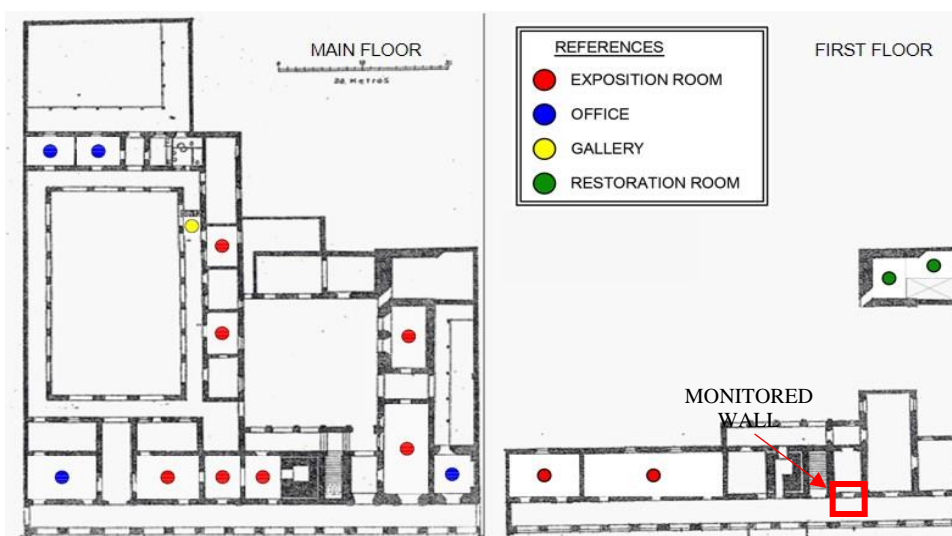


Fig. 2. Plan view of the building.

## Methodology

### *Historical data survey*

First, a historical survey of the Cabildo of Salta was carried out to compile the information from previous studies and the written and graphic documents from historical archives. The scarce documentary data available is scattered in public archives and national and provincial libraries. This information was complemented with an in-situ survey of the place. Through this survey, it was possible to infer the different phases and construction systems of the building. However, the spatial distribution of such systems could not be precisely determined due to the lack of records,

nor could it be visually established because the wall surfaces of the building are fully plastered. Previous studies mention at least three distinct constructive systems coexisting in the Cabildo: adobe, stone, and brick masonry. With this information, the probable configurations of such constructive systems, which were preserved during the 1940 restoration campaign, were analyzed as well as the new systems that were likely incorporate during the restoration.

#### ***Thermographic survey***

A thermographic study of the Cabildo was carried out on March 14<sup>th</sup> and 15<sup>th</sup> of 2018. The exterior walls of the building were inspected with a FLUKE Ti 55 thermographic camera [38]. This camera has a spectral band between 8 and 14 $\mu$ m, a resolution of  $\pm 2^{\circ}\text{C}$ , and can simultaneously record infrared and visible spectrum images. The post-processing of the infrared images was performed with the thermal imaging software Fluke SmartView R&D [38]. The thermographic survey was conducted in the afternoon time to allow the walls to warm up enough during the day due to solar radiation, thus enhancing the thermographic detection. Thermal images were acquired in those areas where the constructive component could be qualitatively identified. The collected thermographic imagery was the base to roughly estimate the percentage material composition of the walls, a key piece of information required for realistic simulation of the thermal building behavior.

The weather conditions during the thermographic survey were monitored from a Davis Vantage Pro II Weather Station [39] located at the Universidad Nacional de Salta, approximately 10km away from the Cabildo. Air temperature and humidity, solar radiation on a horizontal surface, and wind direction and velocity were registered. During the first day of the survey campaign, the sky was partially clouded (no rainfalls recorded). During the second day, the sky was mostly clear (the recorded solar radiation at the solar noon was  $900\text{W}/\text{m}^2$ ) with some occasional clouds. The exterior air temperature during the two days oscillated between 19 and  $28^{\circ}\text{C}$ .

#### ***In-situ wall thermal monitoring and determination of the thermal resistance R and the thermal capacity C***

The methodology employed for the thermal characterization of the wall materials of the Cabildo consisted of a combination of in-situ temperature and heat flux measurements with dynamical characterization methods. Through this methodology, it is possible to obtain an estimation of the thermal resistance R and the thermal capacitance C.

#### ***In-situ measurement set-up***

The methods for the estimation of the thermal properties of the wall, which are described in the following sections, require the measurement of the internal and external surface temperatures and the heat flux through the wall, during a period of several days. To monitor these variables, two temperature and one heat flux sensors were installed on one of the walls of the investigation and extension room, on the second floor of the Cabildo (Fig. 2). The wall where the sensors were placed is 0.642m thick with its exterior side facing south, to an internal gallery (Fig. 3). Hence, that side of the wall does not receive direct solar radiation, as suggested in the literature in order to minimize possible solar influence. The wall material is unknown and, based on historical data, it is presumed that this wall, together with the other walls of this wing of the building (the oldest one), are made of adobe. The measurement campaign was carried out during the winter dry season, between July 2<sup>nd</sup> and July 31<sup>th</sup>, 2019.

The interior and exterior surface temperatures of the wall were measured with two K-type calibrated thermocouples connected to an Onset HOBO U12-014 thermocouple datalogger (12-bit, resolution  $0.32^{\circ}\text{C}$  at  $625^{\circ}\text{C}$ , accuracy  $\pm 4.0^{\circ}\text{C}$  or 0.5% of reading, whichever is greater) [40]. The sampling period was 15 minutes. The optimal placement of the sensors was deemed to be the geometrical center of a brick. The infrared camera Fluke Ti 55 was used to visualize the brick layout of the wall and choose the desired location. The heat flux through the wall was measured with a Hukseflux HP01 heat flux plate sensor (nominal sensitivity  $61.26\text{mV}\cdot\text{W}^{-1}\cdot\text{m}^2$ ) [41] connected to a NOVUS data acquisition system LOGBOX-AA IP65. The sensor was tightly

attached to the inner side of the test wall with adhesive tape. The heat flux through the wall is usually measured at the inner side where the heat flux is more stable than at the outdoor side. The flow meter was installed approximately 20 mm away from the mortar joint edge, as suggested by Meng *et al.* [42]. Outdoor environmental conditions (air temperature, relative humidity, wind velocity and direction, and solar irradiance on the horizontal surface) during the whole measurement period were monitored with the aforementioned wireless Davis Vantage Pro II Weather Station [39].



**Fig. 3.** Pictures of the Cabildo of Salta: a) North façade; b) external side of the monitored wall; c) internal side of the monitored wall.

#### *Method for the determination of the thermal resistance $R$*

The thermal resistance  $R$  can be defined as the temperature difference across a wall that produces a unit heat energy flux through it in unit time in quasi-steady conditions. For a homogeneous wall with uniform surface temperatures  $T_{in}$  and  $T_{ex}$  a unidimensional heat flow can be assumed and the thermal resistance can be determined as follows:

$$R = \frac{(T_{in} - T_{ex})}{q_{in}} \quad (1)$$

where  $T_{in}$  and  $T_{ex}$  are the (constant) internal and external wall surface temperatures and  $q_{in}$  is the (constant) heat flux measured on the interior side of the wall. In the case that a wall is made up of multiple layers of different materials, the equivalent thermal resistance can be calculated as the sum of the individual thermal resistance of each layer.

Apart from controlled laboratory conditions, steady-state conditions are practically impossible to achieve in real scenarios where the walls of a building may be subjected to outdoor weather conditions. For this reason, quasi-steady methods, such as the average method ISO 9869 [43], were developed. The average method has become the most widely accepted method for the onsite thermal characterization of building elements. It relies on the fact that the time-averaging of the measured temperatures and the heat fluxes during long periods cancels out the transient effects. This method works well if the outdoor temperature is always lower (or higher) than the indoor temperature and if the measuring period is long enough. Usually, a difference between the outdoor and indoor temperature larger than 10°C is recommended together with a one-directional heat flux requirement. These conditions could be achieved in artificially heated buildings. But, preserved historic buildings are most likely non-conditioned free-running buildings with no installed HVAC systems. Hence, room temperatures cannot be directly controlled to meet the requirements of the quasi-steady methods. Therefore, the usually low thermal gradient between the outdoor and indoor wall conditions than can be obtained in free-running buildings preclude the use of quasi-steady methods due to convergence issues (the predicted value of  $R$  does not converge as the dataset becomes longer). For this reason, dynamical characterization methods were introduced to overcome the mentioned drawback.

In this paper, the dynamic Pentaur Method [44] was used as a first alternative to estimate the thermal resistance R from the measurement data. This method was showed to have a good performance for the prediction of the thermal resistance under dynamic free-running conditions with alternating heat flux [45, 46]. The Pentaur model belongs to the category of autoregressive statistical methods with exogenous input variables (ARX) and was developed in base of physical and statistical grounds. The method proposes that the instantaneous heat flux through a building constructive component depends on four different contributions: the past fluctuations of the heat flux between consecutive times, the steady-state component of the heat flux, and the fluctuations between consecutive times of the internal and external temperatures. Mathematically, the heat flux density at a time  $t_p$  is expressed as follows:

$$q_{in,p} = \frac{(T_{in,p} - T_{ex,p})}{R} + \sum_{n=j}^k dT_{in,n}A_n + \sum_{n=j}^k dT_{ex,n}B_n + \sum_{n=j}^k dq_{in,n}C_n, \quad (2)$$

where:  $k = p-1$  is the number past “time steps” and  $j$  is such that  $t_p - t_j$  is equal to the influence time (between 12 and 48 h),  $T_{in,p}$  and  $T_{ex,p}$  are the internal and external wall face temperatures at time  $t_p$ , respectively, and  $dT_{in,n}$  (°C),  $dT_{ex,n}$  (°C) and  $dq_{in,n}$  (Wm-2) are the changes in the internal and external wall face temperatures, and in the heat flux density on the interior face of the wall, respectively, between two consecutive time steps  $t_{n-1}$  and  $t_n$ , that is to say,

$$\begin{aligned} dT_{in,n} &= T_{in,n} - T_{in,n-1}, \\ dT_{ex,n} &= T_{ex,n} - T_{ex,n-1}, \\ dq_{in,n} &= q_{in,n} - q_{in,n-1} \end{aligned} \quad (3)$$

The parameters in Eq. (2) are  $R^{-1}$ ,  $A_n$ ,  $B_n$ , and  $C_n$  (1+3(k-j+1) parameters). These parameters, the coefficients of a multilinear regression, were estimated through least square minimization of residuals [47]. *Anderlind* (1996 and 2017) [48, 49] showed that the Pentaur method is effective in the majority of experimental scenarios, even for massive multi-layered walls or for cases where the heat flux is relatively small, for example during the summer periods.

In the present effort, the following convergence criteria based on the coefficient of variation CV or relative standard deviation is adopted. The estimated value of R is said to converge at a time  $t_c$  (convergence time) when the CV of the data subset ranging from 24h before to 24h after (48h time interval) the time  $t_c$  is smaller than 3% and the CV during the previous 72h to  $t_c$  is smaller than 5%. The Pentaur method was implemented computationally using Python 3.6 programming language.

Once the convergence criteria are met for the measurement data corresponding to the time  $t_c$ , the estimation process for R (and the coefficients  $A_n$ ,  $B_n$ ) through Eq. (2) is stopped. The remaining of the collected data from the time  $t_c$  on are used as a validation data set to evaluate the precision of the statistical model with the estimated fixed parameters. The goodness of the fit between the predicted values and the validation data is analyzed in terms of the following statistical indicators: normalized root mean square error (NRMSE), correlation coefficient (Corr), and standard deviation ratio (STDr). These statistics are defined in the Eqs. (4) to (6).

$$NRMSE = 1 - \sqrt{\frac{\sum_{i=1}^N (y_i - x_i)^2}{\sum_{i=1}^N (y_i - \bar{y})^2}} \quad (4)$$

$$Corr = \frac{\sum_{i=1}^N (y_i - \bar{y})(x_i - \bar{x})}{N\sigma_x\sigma_y} \quad (5)$$

$$STDr = \frac{\sigma_x}{\sigma_y} \quad (6)$$

where:  $\bar{y}$  and  $\bar{x}$  and  $\sigma_x$  and  $\sigma_y$  are the mean and the standard deviation values of the prediction  $x_i$  and measured  $y_i$  validation data set, respectively.

*Alternative method for the determination of both the thermal resistance and the thermal capacitance C*

The thermal capacitance  $C$  is defined as the heat flow necessary to change the temperature rate of a medium by one unit in one second. This property is related to the energy storage capacity or thermal inertia of the material. For a homogeneous slab with density  $\rho$ , specific heat  $c_p$ , and thickness  $e$ , the thermal capacitance is defined as:

$$C = \rho c_p e \tag{7}$$

Models based on the analogy between heat transfer phenomenon and the charge flow in electrical RC circuits provide a simple description and interpretation of the heat transfer in a system. These equivalent electrical circuits include resistors (analogous to the thermal resistance) and capacitors (analogous to the heat capacity) arranged in different configurations to better represent the heat transfer paths. The simplest configuration to describe the thermal behavior of a homogeneous wall is an R2C network. This model is depicted in figure 4.

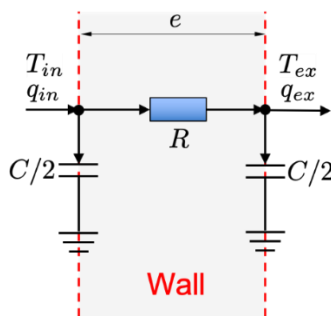


**Fig. 4.** R2C electrical circuit to characterize the heat transfer phenomenon through a simple wall (Seem 1987)

In the present article, a wall with thickness  $e$  [m], thermal conductivity  $k$  [ $\text{W}\cdot\text{m}^{-1}\cdot\text{K}^{-1}$ ], mass density  $\rho$  ( $\text{kg}\cdot\text{m}^{-3}$ ), and specific heat capacity  $c_p$  [ $\text{J}\cdot\text{kg}^{-1}\cdot\text{K}^{-1}$ ] is represented by two nodes (one on each face of the wall), connected to a grounded capacitor  $C/2 = \rho c_p e/2$  [ $\text{J}\cdot\text{m}^{-2}\cdot\text{K}^{-1}$ ], and a single resistor  $R = \frac{e}{k}$  [ $\text{m}^2\cdot\text{K}\cdot\text{W}^{-1}$ ] connecting these nodes. This model can also be obtained from the one-dimensional heat equation through the semi-discrete approach (method of lines). If a finite difference discretization is applied to the spatial derivative of the heat flux  $\partial q/\partial x$  in the one-dimensional heat equation using only an interior node and two exterior nodes, one on each face of the wall, it is possible to show that the time rate of change of the temperature on one of the wall faces (in this case, the internal face, where the heat flux was measured) is given by:

$$\frac{dT_{in}}{dt} = -\frac{T_{in} - T_{ex}}{RC/2} + \frac{q_{in}}{C/2} \tag{8}$$

This equation determines the mathematical structure of the model but contains the unknown parameters  $R$  and  $C = \rho c_p e$ , which can be estimated through the fit of the model given by Eq. (8) to the measurement data. Therefore, this approach constitutes a Grey Box or Semi-Physical Model. In Eq. (8), the independent variable is  $T_{in}$ , and the dependent (input) variables are  $T_{ex}$  y  $q_{in}$ . This approach differs from the Pentaur method previously described, which estimates  $q_{in}$  instead of  $T_{in}$ .

It is noted that the present strategy will produce different estimations of  $R$  and  $C$  depending on the length of the measurement dataset used. Therefore, it is possible, as it was with the Pentaur method, to obtain a plot of  $R$  and  $C$  as a function of the elapsed time of the dataset. To make the

comparison between the methods meaningful, the same convergence criteria used for the Pentaur method is adopted in this case.

Similarly to the Pentaur methods, once the convergence is reached, the remaining data is used as a validation dataset. The goodness of the fit between the predicted values and the validation data is analysed, as in the case of the thermal resistance, through the normalized root mean square error (NRMSE), correlation coefficient (Corr), and standard deviation ratio (STDr), previously defined in equations (4), (5) and (6).

**Derivation of other thermal properties**

With the estimated thermal resistance  $R$  and the thermal capacity  $C$  values, other thermal properties of the element of interest can be determined. These properties are described in the following sections.

*Static thermal transmittance*

The calculation procedure for the steady-state air-to-air thermal transmittance, or  $U$ -value [ $\text{W}\cdot\text{m}^{-2}\cdot\text{K}^{-1}$ ], is described in the standard ISO 13786 [50]:

$$U = \frac{1}{R_{s,ext} + R + R_{s,int}} \tag{9}$$

where  $R$  is the thermal resistance of the wall [ $\text{m}^2\cdot\text{K}\cdot\text{W}^{-1}$ ],  $R_{s,ext}$  and  $R_{s,int}$  [ $\text{m}^2\cdot\text{K}\cdot\text{W}^{-1}$ ] are the external and internal surface resistances, respectively. These two variables have standardized values of 0.04 and 0.13  $\text{m}^2\cdot\text{K}\cdot\text{W}^{-1}$ , respectively.

*Thermal conductivity, effusivity, and diffusivity*

The effective thermal conductivity  $\lambda$  [ $\text{W}\cdot\text{m}^{-2}\cdot\text{K}^{-1}$ ] can be estimated from the thermal resistance  $R$  and the total thickness of the wall  $e$  [m]:

$$\lambda = \frac{e}{R} \tag{10}$$

The thermal storage efficiency is a function of a material's properties: specific heat, apparent density, and thermal conductivity. These three material parameters may be combined into one called thermal effusivity  $\varepsilon$  [ $\text{J}\cdot\text{s}^{1/2}\cdot\text{m}^{-2}\cdot\text{K}^{-1}$ ].

$$\varepsilon = \sqrt{\lambda\rho c_p} \tag{11}$$

The thermal diffusivity  $\alpha$  [ $\text{m}^2/\text{s}$ ], a variable related to the velocity of propagation of the heat wave, is defined as:

$$\alpha = \frac{\lambda}{\rho c_p} \tag{12}$$

**Results**

**Identification of materials through infrared inspection**

A few of the thermal images collected of the Cabildo envelope are shown in Figures 5 and 6. From the different constructive components, stone is usually recognized because of on its rounded geometry (rounded quadrangular blocks) and its rather irregular dimensions (approximately 0.27x0.30m). Based on the infrared images, it is inferred that stone was primarily used for the construction of the main façade facing the street: in the arcade on the ground floor, in the pillars of both floors, and in the area near the doors of the exterior walls (Fig. 5). In the interior of the building, stone was used to construct the walls of the South wing facing the main courtyard.

Adobe bricks can be identified in the thermal images because they are usually regular blocks elements with average heights of 0.10m, but with variable widths (Fig. 5). It is inferred from the infrared images that adobe was primarily used in the construction of the walls and arcs of the first floor, which are thicker and larger, respectively, than those of the main floor. It is hypothesized that such a choice was due since adobe bricks are usually much lighter than stones. The identified adobe bricks are about 0.51-0.55m long and 0.10m thick. Finally, massive ceramic bricks were also recognized based on their smaller dimensions (de 0.33-0.35m x 0.08m). They were identified mainly under the cornice of the main façade.

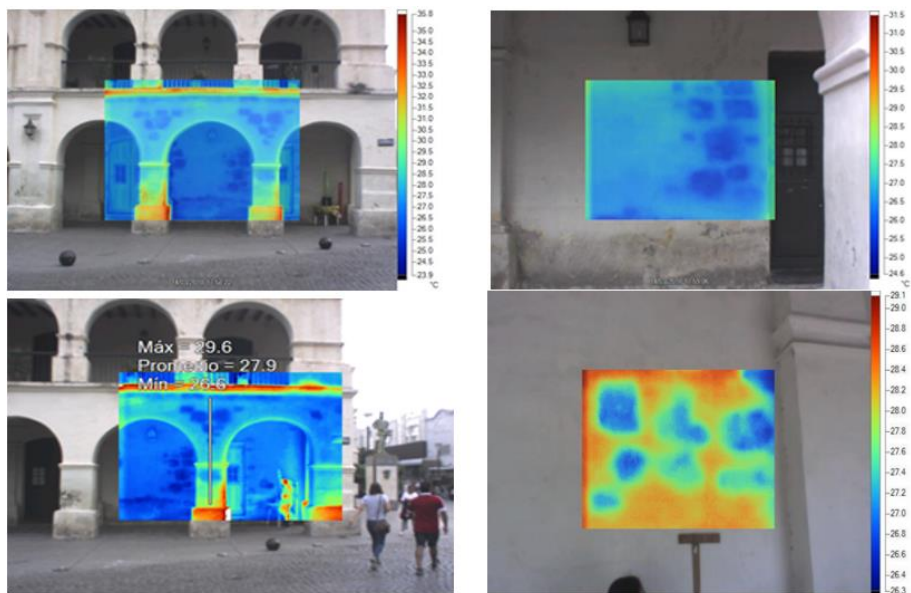


**Fig. 5.** Infrared images showing the irregular shape of the stones used in the arcs of the gallery and in the areas close to the doors

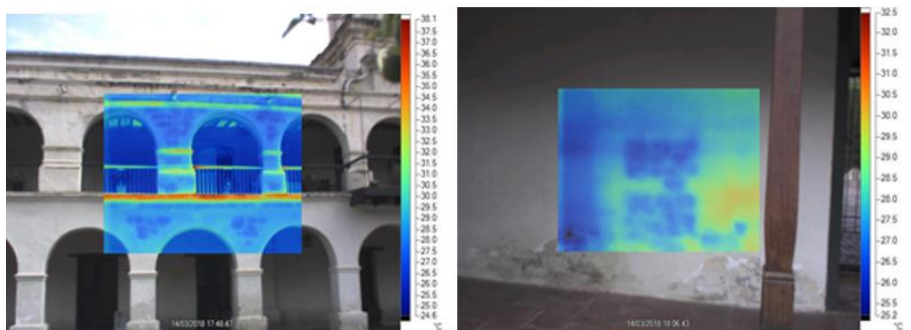


**Fig. 6.** Infrared images showing adobe bricks in the arcades of the first floor (left) and in the walls of the West façade (right). Massive ceramic bricks were used in the decorative comices above the arcs

Based on the thermal images collected, the available compiled historical data and information, and visual inspections, a stratigraphy of the main façade was elaborated (Figs. 7 and 8) identifying the most probable configuration of materials on the Cabildo walls (Table 1).

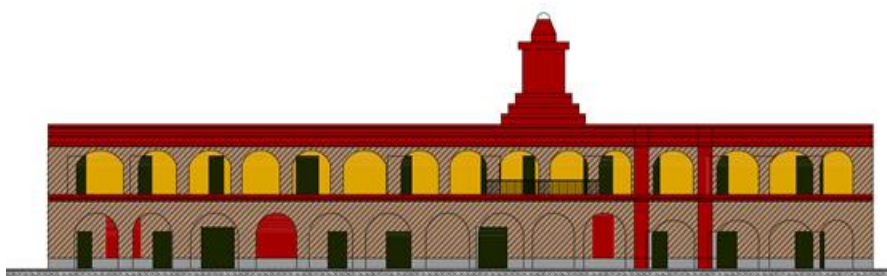


**Fig. 7.** Stratigraphy of the main façade (North) of the Cabildo of the city of Salta

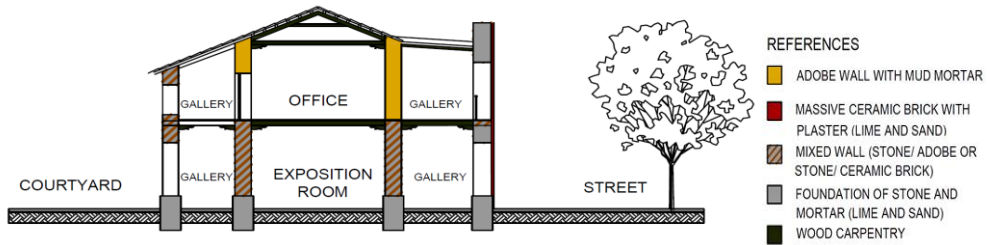


Fig. 8. Stratigraphy of the Cabildo of the city of Salta. Cross view (East-West)

Table 1. Description of the constructive elements of the Cabildo of the city of Salta

Element	Description	
Foundations	Stone with joining mortar. Height: 0.50-0.80m above the ground level	
Walls	Type 1 Adobe plastered on both sides with mud mortar. Thickness: 0.60-0.70m	
	Type 2 Mix of stone and adobe	Thickness: 0.83 – 1.10m (façade) 0.70m (interior walls)
	Type 3 Mix of stone and solid ceramic brick	
Floor (First floor)	Wood structure with ceramic tile covering	
Roof	Wood structure with ceramic tiles	
Arcs (façade and courtyards)	Type 1 Stone (details and molding of plastered solid bricks)	
	Type 2 Solid bricks in the arcs of the main courtyard (Gómez R., 1999)	

**Determination of the thermal resistance *R* and the thermal capacitance *C***

*In situ thermal behaviour monitoring of a wall*

One wall of the original building, presumably built with adobe bricks, was selected to be studied. This wall is external and belongs to a room on the first floor. It was selected because it is directly exposed to the outdoor air conditions and also because it is shaded from solar irradiation. These conditions are likely to produce acceptable, large enough temperature differences between the opposite faces of the wall, following the requirement of the methods for estimation of the *R*-value. The time history of the weather conditions (air temperature and solar global irradiance on a horizontal surface) recorded during the measurement period in July of 2019 (31 days) are summarized in figure 9. Keeping track of the weather conditions is important because unexpected meteorological phenomena (cold air fronts, heat waves, and so on) can deter the convergence of the dynamic estimation methods. During the measurement period, the air temperature experienced wide variations between 0 and 32°C, with mean daily thermal amplitudes on sunny days of approximately 20°C. A noticeable change in the meteorological conditions is observed starting on July 22<sup>nd</sup>. A strong drop in the air temperature right after the hottest day of the month was registered. This event is highlighted because it was picked up by the estimation methods as a change in the predicted values of *R*. As the radiation data in figure 7 suggest, the days during the monitoring were mostly sunny, with clear skies and low cloudiness. Only a few periods of cloudy days were registered (on July 4-6, 13, 15-16, and 23-25). As it was already stated in the methodology section, these highly variable outdoor conditions are not suited for quasi-steady thermal resistance estimation methods; thus, dynamical methods are the best option in this case.

The recorded time history of the wall internal and external surface temperatures,  $T_{in}$  and  $T_{ex}$ , respectively, and the heat flux through the wall  $q_{in}$  are presented in figure 10. The total number of sampled data points is 2950. Considering the sampling period of 15min, the data corresponds to roughly 30 continuous days worth of measurements. For the reasons mentioned in the previous paragraph and to aid the convergence of the thermal resistance estimation methods, the initial

period of six days was disregarded. Besides, the unusually large difference between internal and external wall surface temperatures lead us to believe that an auxiliary small heating device was most likely turned on during this period. From July 7<sup>th</sup> on, the office room was lightly occupied and no heaters were used. Therefore, the data collected from that day on suits the conditions of a free-running building wall. It is important to mention that the unsupervised monitoring activities did not interfere with the normal daily use of the building and its spaces.

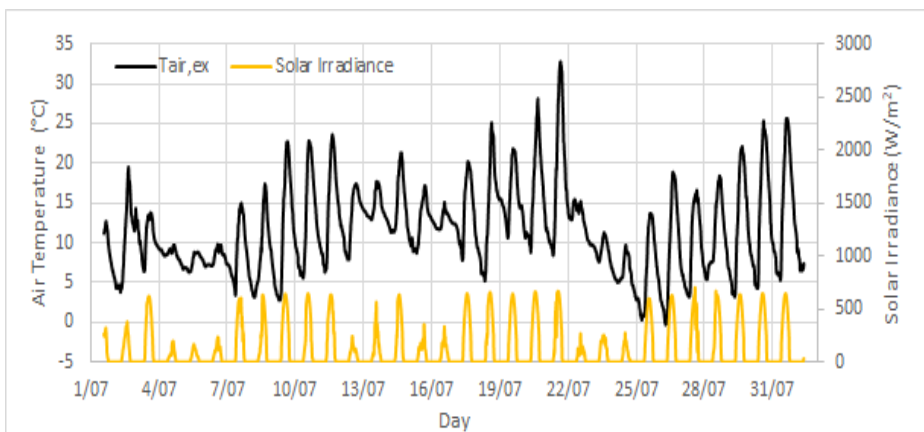


Fig. 9. Weather conditions (air temperature and global solar irradiance on a horizontal surface) during the measurement period

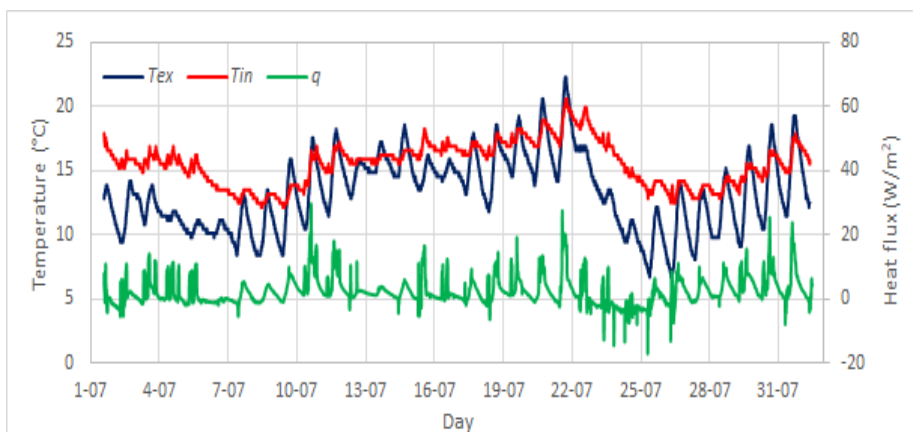
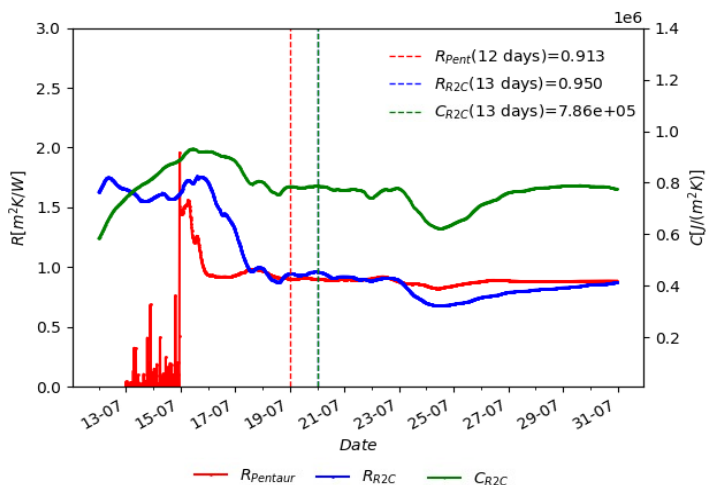


Fig. 10. Time history of the monitored variables. Primary (left) axis: temperatures on the internal and external surfaces of the wall. Secondary (right) axis: heat flux rate measured on the internal face of the wall

#### Estimation of Thermal Properties $R$ and $C$

The Pentaur method and the R2C model are employed to obtain estimations of the thermal resistance and thermal capacitance of the monitored wall. Following the methodology described in Section 3.3, an estimation of the value of  $R$  can be obtained as a function of the amount of measurement data points used for the estimation. Because of the reasons mentioned in the previous section, measurement data up until the end of July 6<sup>th</sup> was disregarded for the computation of  $R$  and  $C$ . The values of  $R$  estimated through each of the models as a function of the measurement time is shown in figure 11. The large fluctuations in the values of  $R$  (and  $C$ ) estimated by the models between July 22<sup>nd</sup> and 26<sup>th</sup> are due to the aforementioned abrupt changes in the meteorological conditions during those days. The estimated values of  $R$  and  $C$  from July

7<sup>th</sup> to July 12<sup>th</sup> were not included in figure 11 because they presented fluctuations that are much larger than the scale of the plots.



**Fig. 11.** Evolution of the values of the thermal resistance  $R$  and capacitance  $C$  estimated by the in-situ measurements. The vertical dashed lines indicate the day at which the convergence criteria were satisfied by each method

A summary of the results obtained with both methods is presented in Table 2. In this table, the values  $R(t_c)$  and  $C(t_c)$  are the values obtained at the time  $t_c$  when the convergence criteria is met. Also, the mean and standard deviation values of  $R$  and  $C$  over a period of 3 days centered at the time of convergence are reported in the table. The Pentaur model met the convergence criteria after 12 days worth of data to a value of  $R = 0.91\text{m}^2\cdot\text{K}\cdot\text{W}^{-1}$ . For this model, a 48-hour influence window was used; therefore, a total of 577 coefficients ( $1 + 3 \times 4 \times 48$ ) were estimated. Other influence windows with 24 and 36 hours were tested, but the 48-hour window was finally chosen because it leads to a better correlation and NRMSE of the validation data (Table 3). The R2C model converged after 13 days to values of  $R = 0.95\text{m}^2\cdot\text{K}\cdot\text{W}^{-1}$  and  $C = 7.86 \times 10^5\text{J}/(\text{m}^2 \cdot \text{K})$ . The value of the Pentaur coefficients  $A_n$ ,  $B_n$ , and  $C_n$  (577 in total) are not included in the summary because they lack physical interpretation.

**Table 2.** Summary of the results of the Pentaur and R2C methods

	$R$ ( $\text{m}^2\text{K}/\text{W}$ )			$C$ ( $\text{J}/\text{m}^2\text{K}$ )			$t_c$ (days)
	$R(t_c)$	3-day Mean	3-day STD	$C(t_c)$	3-day Mean	3-day STD	
R2C	0.95	0.95	0.048	$7.86 \times 10^5$	$7.88 \times 10^5$	$1.7 \times 10^4$	13
Pentaur	0.91	0.95	0.047	-	-	-	12
	$R = 0.93 \pm 0.05$			$C = (7.9 \pm 0.2) \times 10^5$			

The validation of the models with estimated (and now fixed) values of  $R$ ,  $A_n$ ,  $B_n$  and  $C_n$  for the Pentaur model and  $R$  and  $C$  for the R2C model is performed using the remaining of the measurement data from the day of convergence onwards. The corresponding independent variable (heat flux rate  $q_{in}$  for the Pentaur and internal wall surface temperature  $T_{in}$  for the R2C model) was predicted with each model, and these predictions were compared with the actual measurement data. The comparison between the predicted history of the heat flux rate (for Pentaur method) and internal wall face temperature (for R2C model) and the actual data is shown in figure 10. The statistical error analysis for the predicted data is summarized in Table 3. It is observed in Fig. 12a that the Pentaur model with the estimated thermal resistance value of  $0.91\text{m}^2\cdot\text{K}\cdot\text{W}^{-1}$  predicts quite well the measurement data after the convergence point. The mean of the error of

the prediction of this model is  $0.23\text{W}\cdot\text{m}^{-2}$ , with the largest errors occurring between July 22<sup>nd</sup> and July 26<sup>th</sup> when significant variations in the weather conditions were registered. It is observed in figure 12b that the R2C model can capture the main trend of the internal wall face temperature variation but not the details (that is to say, it is missing the high-frequency components). However, the performance of the model is still quite acceptable as judged by the correlation and standard deviation ratios which are close to 1.

Finally, the range of probable values of  $R$  and  $C$  is provided in Table 2. For  $R$ , an average of the two methods was performed. Thus, the estimated values are  $R = (0.93 \pm 0.05)\text{m}^2\text{K}/\text{W}$  and  $C = (7.9 \pm 0.2) \times 10^5\text{J}/\text{m}^2\text{K}$ .

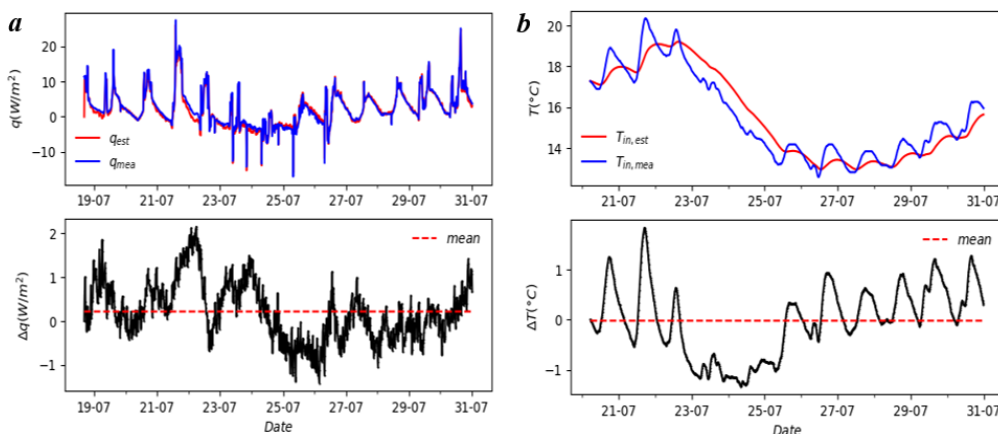


**Fig. 12.** Comparison between measurement data and predicted values. a) Heat flux rate predicted with Pentaur method (red line). b) Internal wall face temperature estimated through the R2C model (red line). Measured data are shown with a blue line

**Table 3.** Statistical error analysis for the predictions of Pentaur and R2C methods

	Parameters	NRMSE	Corr	STDr
R2C	2	0.70	0.94	1.03
Pentaur	577	0.86	0.99	0.99

**Derivation of other thermal properties**

Once the thermal resistance and capacitance were determined together with the wall thickness ( $e = 0.642\text{m}$ ), the additional thermal properties of the monitored wall were determined through Eqs. (8) to (11). The corresponding errors were determined by the usual calculation of error propagation. The results are summarized in Table 4.

**Table 4.** Additional thermal properties of the wall.

	Estimated value
Static thermal transmittance $U$	$0.91 \pm 0.06\text{W}/(\text{m}^2\cdot\text{K})$
Effective thermal conductivity $\lambda$	$0.69 \pm 0.04\text{W}/(\text{m}\cdot\text{K})$
Effective thermal effusivity $\varepsilon$	$919 \pm 40\text{J}/(\text{s}^{1/2}\cdot\text{m}^2\cdot\text{K})$
Effective thermal diffusivity $\alpha$	$5.64 \pm 0.5 \times 10^{-7}\text{m}^2/\text{s}$

The values obtained for the thermal conductivity ( $\lambda = 0.69\text{W}\cdot\text{m}^{-1}\cdot\text{K}^{-1}$ ) and capacitance ( $C = 7.9 \times 10^5\text{J}/\text{m}^2\cdot\text{K}$ ) are in line with values for adobe found by other researchers. Reported values for the thermal conductivity of adobe usually range from  $0.30$  to  $1.54\text{W}/(\text{m}\cdot\text{K})$ , depending on its density and its water content, amongst other factors [33, 51, 52]. In the case of dry adobe, typical values found in the literature are between  $0.56$  and  $0.80\text{W}/(\text{m}\cdot\text{K})$  [31]. On the other hand, the reported values of the thermal capacitance  $C$  of adobe walls range between  $4.7$  and  $10.9 \times 10^5\text{J}\cdot\text{m}^{-2}\cdot\text{K}$ , the density between  $1300$  and  $1700\text{kg}\cdot\text{m}^{-3}$ , and the heat capacity between  $559$  and  $1000\text{J}\cdot\text{kg}^{-1}\cdot\text{K}^{-1}$  [30]. It is important to note that actual adobe constructions have wet-dry cycles

due to rain and relative humidity that cause variations of their thermal properties [51]. Additionally, the water contained in the adobe increases its latent heat content and modify both the thermal conductivity and thermal capacity of the material [33].

Based on the previous discussion, it is concluded that the obtained results of  $R$  and  $C$ , the dimensions of the bricks observed through the thermographic analysis, and the historic data, all provide strong evidence that adobe is most likely the material used for the construction of the wall under analysis.

## Conclusions

The energy retrofit of historic buildings is in the focus of current research at the international level. One of the main issues in this field is the estimation of the thermal properties of the building walls through non-destructive, in situ measurements. The estimation of these parameters is of uppermost importance for increasing the reliability of the results obtained through the energy simulation models. In this paper, the masonry patterns and the thermal properties of an adobe wall of the colonial Cabildo of the city of Salta (Argentina) were characterized using two in-situ non-destructive methods complemented with information from historic archives. Infrared thermography and dynamical wall surface temperatures and heat flux rate measurements were used to determine the thermal resistance, transmittance, conductivity, thermal capacity, and thermal diffusivity of one of the walls of the building.

Infrared thermography provided excellent results in sunny walls. The different thermal and geometrical characteristics of the wall components (adobe blocks, stone, ceramic, and joining mortar) allowed them to be identified through the thermal images where the shape of the components was clearly visible. Regular blocks were hypothesized to be adobe or massive ceramic bricks, while irregular elements were assumed to be stone. The historic sources confirmed some of the obtained results; thus, for the first time, a stratigraphy of the main façade of the Cabildo was composed. The thermal resistance and capacitance of an exterior wall were estimated through experimental measurements of the heat flux rate and the wall surface temperatures, and the dynamical Pentaur and R2C characterization models. The values obtained for the thermal conductivity ( $\lambda = 0.69 \text{ W} \cdot \text{m}^{-1} \text{ K}^{-1}$ ) and capacitance ( $C = 7.9 \times 10^5 \text{ J} \cdot \text{m}^{-2} \text{ K}^{-1}$ ) are in agreement with values found by other researchers for adobe bricks. Therefore, it is concluded that the methods presented were successful in determining these variables and that their application can be potentially extended to other elements of the building envelope and other heritage buildings in different environmental contexts. In particular, future works in this direction should focus on analysing the suitability of the dynamical estimation methods for walls made of different materials, for buildings under different climates and/or measurements performed during different seasons from the one studied in the present effort (winter). The obtained results provide scientific support for decision making in future energy retrofit strategies and restoration of heritage buildings where the use of destructive study methods should be avoided.

## Acknowledgments

This research was supported by the National University of Salta and ANPCYT (National Agency of Scientific and Technological Promotion). The authors want to express their gratefulness to Arq. Carola Herr for her valuable help in providing documentary sources and historic information of the building, to Arq. Mario Lazarovich (Director of the North Historical Museum), Arq. María Campero de Larrán (curator of the Cabildo of Salta) and to the Museum staff for their excellent predisposition and collaboration in the building monitoring.

## References

- [1] A. Galatioto, R. Ricciu, T. Salem, E. Kinab E. *Energy and economic analysis on retrofit actions for Italian public historic buildings*, **Energy**, **176**, 2019, pp. 58–66. <https://doi.org/10.1016/J.ENERGY.2019.03.167>.

- [2] L. De Santoli, *Guidelines on energy efficiency of cultural heritage*, **Energy and Buildings**, **86**, 2015, pp. 534-540, 10.1016/J.ENBUILD.2014.10.050
- [3] A.L. Webb, *Energy retrofits in historic and traditional buildings: a review of problems and methods*, **Renewable and Sustainable Energy Reviews**, **77**, 2017, pp. 748-759, 10.1016/J.RSER.2017.01.145.
- [4] C. Cornaro, V.A. Puggioni, R.M. Strollo, *Dynamic simulation and on-site measurements for energy retrofit of complex historic buildings: villa Mondragone case study*, **Journal of Building Engineering**, **6**, 2016, pp. 17–28. <https://doi.org/10.1016/j.jobe.2016.02.001>.
- [5] \* \* \*, European Commission. *A European Green Deal. Striving to be the first climate-neutral continent*. Available at: [https://ec.europa.eu/info/strategy/priorities-2019-2024/european-green-deal\\_en](https://ec.europa.eu/info/strategy/priorities-2019-2024/european-green-deal_en).
- [6] A.L. Pisello, A. Petrozzi, V.L. Castaldo, F. Cotana, *On an innovative integrated technique for energy refurbishment of historical buildings: Thermal-energy, economic and environmental analysis of a case study*, **Applied Energy**, **162**, 2016, pp. 1313-1322.
- [7] M. Filippi, *Remarks on the green retrofitting of historic buildings in Italy*, **Energy and Buildings**, **95**, 2015, pp. 15-22.
- [8] G. Di Ruocco, C. Sicignano, A. Sessa, *Integrated methodologies energy efficiency of historic buildings*, **Procedia Engineering**, **180**, 2017, pp. 1653 – 1663.
- [9] D. Paoletti, D. Ambrosini, S. Sfarra, F. Bisegna, *Preventive thermographic diagnosis of historical buildings for consolidation*, **Journal of Cultural Heritage**, **14**, 2013, pp. 116–121.
- [10] E. Quagliarini, E. Esposito, A. del Conte, *The combined use of IRT and LDV for the investigation of historical thin vaults*, **Journal of Cultural Heritage**, **14**, 2013, pp. 122–128.
- [11] M.S. Georgescu, C.V. Ochinciuc, E.S. Georgescu, I. Colda, *Heritage and Climate Changes in Romania: the St. Nicholas church of Densus, from degradation to restoration*, **Energy Procedia**, **133**, 2017, pp. 76-85.
- [12] S. Abdelaal, I.C.A. Sandu, *Assessment of protease in cleaning of bat blood patches from ancient Egyptian wall paintings and surface inscriptions*, **International Journal of Conservation Science**, **10**(3), 2019, pp. 459-474.
- [13] E. Lucchi, *Applications of the infrared thermography in the energy audit of buildings: a review*, **Renewable and Sustainable Energy Reviews**, **82**, 2018, pp. 3077–90. <https://doi.org/10.1016/J.RSER.2017.10.031>.
- [14] M. Rotilio, F. Cucchiella, P. De Berardinis, *Thermal transmittance measurements of the historical masonries: some case studies*, **Energies**, **11**(11), 2018, Article Number: 2987.
- [15] R.S. Adhikari, E. Lucchi, V. Pracchi, *Experimental measurements on thermal transmittance of the opaque vertical walls in the historical building*, **Proceedings of the 28th International PLEA Conference**, Lima (2012), 7-9 November 2012.
- [16] D.S. Choi, M.J. Ko, *Comparison of Various Analysis Methods Based on Heat Flowmeters and Infrared Thermography Measurements for the Evaluation of the In Situ Thermal Transmittance of Opaque Exterior Walls*, **Energies**, **10**(7), 2017, Article Number: 1019. DOI 10.3390/en10071019.
- [17] G.G. Akkurt, N. Aste, J. Borderon, A. Buda, M. Calzolari, D. Chung, V. Costanzo, C. Del Pero, G. Evola, H.E. Huerto-Cardenas, F. Leonforte, A. Lo Faro, E. Lucchi, L. Marletta, F. Nocera, V. Pracchi, C. Turhan, *Dynamic thermal and hygrometric simulation of historical buildings: Critical factors and possible solutions*, **Renewable and Sustainable Energy Reviews**, **118**, 2020, Article Number: 109509, <https://doi.org/10.1016/j.rser.2019.109509>.
- [18] B. Gonzalo, F. Estirado, R. Undurraga, J.F. Conde, F. Agua, M.A. Villegas, M. Garcia-Heras, *Brick masonry identification in a complex historic building, the Main College of the University of Alcalá, Madrid (Spain)*, **Construction and Building Materials**, **54**, 2014, pp. 39–46. <http://dx.doi.org/10.1016/j.conbuildmat.2013.12.027>.
- [19] C. González-Longo, D. Theodosopoulos, *Construction and materials in the stratification of S. Maria Nova (S. Francesca Romana) at the Roman Forum*, **Construction and Building Materials**, **41**, 2013, pp. 926–941.
- [20] F. Ascione, F. Ceroni, R.F. De Masi, F. de' Rossi, M.R. Pecce, *Historical buildings: multidisciplinary approach to structural/energy diagnosis and performance assessment*.

- Applied Energy**, **185**, 2017, pp. 1517–1528. DOI: <https://doi.org/10.1016/J.APENERGY.2015.11.089>.
- [21] A. Al-Omari, X. Brunetaud, K. Beck, M. Al-Mukhtar, *Thermal stress and damage risk in the stones of Al-Ziggurat in Al-Nimrud city, Iraq*, **Journal of Cultural Heritage**, **37**, 2019, pp. 9-16, DOI: <https://doi.org/10.1016/j.culher.2018.10.011>.
- [22] E. Lucchi, *Thermal transmittance of historical brick masonries: a comparison among standard data, analytical calculation procedures, and in situ heat flow meter measurements*, **Energy and Buildings**, **134**, 2017, pp. 171–84. <https://doi.org/10.1016/J.ENBUILD.2016.10.045>.
- [23] I. Nardi, E. Lucchi, T. de Rubeis, D. Ambrosini, *Quantification of heat energy losses through the building envelope: a state-of-the-art analysis with critical and comprehensive review on infrared thermography*, **Building and Environment**, **146**, 2018, pp. 190–205. <https://doi.org/10.1016/J.BUILDENV.2018.09.050>.
- [24] G. Desogus, S. Mura, R. Ricciu, *Comparing different approaches to in situ measurement of building components thermal resistance*, **Energy and Buildings**, **43**(10), 2011, pp. 2613-2620. <https://doi.org/10.1016/j.enbuild.2011.05.025>.
- [25] E. Genova, G. Fatta, *The thermal performances of historic masonry: in-situ measurements of thermal conductance on calcarenite stone walls in Palermo*, **Energy and Buildings**, **168**, 2018, pp. 363-373.
- [26] J.C. Reyes, L.E. Yamin, W.M. Hassan, J.D. Sandoval, C.D. Gonzalez, F.A. Galvis, *Shear behavior of adobe and rammed earth walls of heritage structures*, **Engineering Structures**, **174**, 2018, Pages 526-537, <https://doi.org/10.1016/j.engstruct.2018.07.061>.
- [27] M.P. Ciocci, S. Sharma, P.B. Lourenço, *Engineering simulations of a super-complex cultural heritage building: Ica Cathedral in Peru*, **Meccanica**, **53**(7), 2018, pp. 1931-1958. DOI: 10.1007/s11012-017-0720-3.
- [28] R. Aguilar, R. Marques, K. Sovero, C. Martel, F. Trujillano, R. Boroschek, *Investigations on the structural behaviour of archaeological heritage in Peru: From survey to seismic assessment*, **Engineering Structures**, **95**, 2015, pp. 94-111. DOI: 10.1016/j.engstruct.2015.03.058.
- [29] G. Zonno, R. Aguilar, R. Boroschek, P.B. Lourenço, *Analysis of the long and short-term effects of temperature and humidity on the structural properties of adobe buildings using continuous monitoring*, **Engineering Structures**, **196**, 2019, Article Number: 109299, <https://doi.org/10.1016/j.engstruct.2019.109299>.
- [30] G.A. Abanto, M. Karkri, G. Lefebvre, M. Horn, J.L. Solis, M.M. Gómez, *Thermal properties of adobe employed in Peruvian rural areas: Experimental results and numerical simulation of a traditional bio-composite material*, **Case Studies in Construction Materials**, **6**, 2017, pp. 177-191, <https://doi.org/10.1016/j.cscm.2017.02.001>.
- [31] J. Chávez-Galán, R. Almanza, N. Rodríguez, *Experimental Measurements of Thermal Properties for Mexican Building Materials to Simulate Thermal Behavior to Save Energy*, **Proceedings of ISES World Congress 2007** (Editors: Goswami D.Y., Zhao Y.), Springer, Berlin, Heidelberg, 2008. [https://doi.org/10.1007/978-3-540-75997-3\\_89](https://doi.org/10.1007/978-3-540-75997-3_89).
- [32] L.F. Aguirre Castellar, A.A. Arrieta Torres, *Estudio comparativo de las propiedades físicas y mecánicas de los materiales utilizados en la restauración de edificaciones de tipología colonial y republicano en la ciudad de Cartagena*, **Civil Engineering Thesis**, Universidad de Cartagena, Facultad de Ingeniería, Programa de Ingeniería Civil, Cartagena D.T. y C. Bolívar, 2014. Available at: .
- [33] M.L. Parra-Saldivar, W. Batty, *Thermal behaviour of adobe constructions*, **Building and Environment**, **41**, 2006, pp. 1892-1904.
- [34] F. Silvero, S. Montelpare, F. Rodrigues, E. Spacone, H. Varum, *Energy retrofit solutions for heritage buildings located in hot-humid climates*, **Procedia Structural Integrity**, **11**, 2018, pp. 52-59, <https://doi.org/10.1016/j.prostr.2018.11.008>.
- [35] A. Michael, M. Philokyprou, S. Thravalou, I. Ioannou, *The role of adobes in the thermal performance of vernacular dwellings*, **Proc. Terra 2016**, Lyon, France. Available at:

- [https://craterre.hypotheses.org/files/2018/07/TERRA-2016\\_Th-4\\_Art-071\\_Michael\\_corr.pdf](https://craterre.hypotheses.org/files/2018/07/TERRA-2016_Th-4_Art-071_Michael_corr.pdf)
- [36] J. Berger, B. Kadoch, *Estimation of the thermal properties of an historic building wall by combining modal identification method and optimal experiment design*, **Building and Environment**, **185**, 2020, 107065.
- [37] A. Nicolini, *Chapter Los antecedentes: el mundo colonial*, **Patrimonio Arquitectónico Argentino - Memoria del Bicentenario (1810-2010) - Tomo I**. Secretaría de cultura, Presidencia de la Nación. 2010, Pág.22. Available in: [https://issuu.com/minculturaar/docs/tomoi\\_ok/26](https://issuu.com/minculturaar/docs/tomoi_ok/26)
- [38] \* \* \*, Fluke, 2021. <https://www.fluke.com/en-us/product/thermal-cameras/ti55ft>
- [39] \* \* \*, Davies Instruments, 2021. <https://www.davisinstruments.com/vantage-pro2/>. Last accessed: 14/11/2020.
- [40] \* \* \*, Onset, 2021. *HOBO U12-014 datasheet*. Available at: <https://www.onsetcomp.com/datasheet/U12-014>
- [41] \* \* \*, Hukseflux, 2021. *HP01 Datasheet*. Available at: <https://www.hukseflux.com/products/heat-flux-sensors/heat-flux-meters/hfp01-heat-flux-sensor>
- [42] X. Meng, B. Yan, Y. Gao, J. Wang, W. Zhang, E. Long, *Factors affecting the in situ measurement accuracy of the wall heat transfer coefficient using the heat flow meter method*, **Energy and Buildings**, **86**, 2015, pp. 754–765.
- [43] \* \* \*, ISO 9869 (2014). *Thermal Insulation—Building Elements—In-Situ Measurements of Thermal Resistance and Thermal Transmittance*, International Organization for Standardization, Geneva, 2014.
- [44] G. Anderlind, *Multiple Regression Analysis of in situ Thermal Measurements — Study of an Attic Insulated with 800 mm Loose Fill Insulation*, **Journal of Thermal Insulation and Building Envelopes**, **16**(1), 1992, pp. 81-104. DOI: 10.1177/109719639201600109
- [45] S. Flores Larsen, M. Hongn, N. Castro, S. Gonzalez, *Comparison of four in-situ methods for the determination of walls thermal resistance in free-running buildings with alternating heat flux in different seasons*, **Construction and Building Materials**, **224**, 2019, pp. 455–473.
- [46] A. Deconinck, S. Roles, *Comparison of characterization methods determining the thermal resistance of building components from onsite measurements*, **Energy and Buildings**, **130**, 2016, pp. 309-320. <https://doi.org/10.1016/j.enbuild.2016.08.061>.
- [47] E. Coelho Barros, P. Angeloti, J. Achcar, E. Zangiacomi, A.C. Shimano, *Métodos de estimação em regressão linear múltipla: aplicação a dados clínicos*, **Revista Colombiana de Estadística**, **31**(1), 2008, pp. 111-129.
- [48] G. Anderlind, *GullfibR and Pentaur Models Two Models for Analysing In Situ Thermal Measurements on a Construction with One-dimensional Heat Flow*, **Proceedings of Building Physics'96**, Espoo, Finland, September 9-10, 1996.
- [49] G. Anderlind, *Comparison of two methods for analyzing in situ thermal measurements*, 2017. [https://www.researchgate.net/publication/318307463\\_Comparison\\_of\\_two\\_methods\\_for\\_Analyzing\\_In\\_Situ\\_Thermal\\_Measurements](https://www.researchgate.net/publication/318307463_Comparison_of_two_methods_for_Analyzing_In_Situ_Thermal_Measurements).
- [50] \* \* \*, *Thermal performance of building components — Dynamic thermal characteristics — Calculation methods*, ISO 13786. European Standard 2017.
- [51] J.D. Revuelta-Acosta, A. Garcia- Diaz, G.M. Soto- Zarazua, E. Rico- Garcia, *Adobe as a Sustainable Material: A Thermal Performance*, **Journal of Applied Sciences**, **10**, 2010, pp. 2211-2216.
- [52] S. Goodhew, R. Griffiths, *Sustainable earth walls to meet the buildings regulations*, **Energy and Buildings**, **37**, 2005, pp. 451-459.

---

Received: February 3, 2021

Accepted: October 2, 2021